SAN099-0172J

Abstract no. -349 Program no. - PS2-MoA2

Ion and Neutral Species in C_2F_6 and CHF_3 Dielectric Etch Discharges+

RaviPrakash Jayaraman, Robert T. McGrath, and Greg Hebner#

227 Hammond Bldg., The Pennsylvania State University, University Park PA 16802

#P.O. Box 5800, Sandia National Laboratories, Albuquerque, New Mexico.

Abstract

Relative concentrations of reactive ions, neutral radicals, resist and substrate etch products have been measured in dielectric etch chemistries using an uncollided beam mass spectrometer / ion extractor from Hiden Analytical. Analysis techniques employed include both electron impact ionization and dissociative ionization of neutral gas, and potential bias extraction of positive ions from the reactor discharge volume. Measurements were made in C_2F_6 and CHF_3 discharges in an inductively coupled plasma (ICP-GEC) research reactor operating with power densities, pressures, gas compositions and wafer materials typical of those found in etch processing tools. Wafer substrates investigated included blanket silicon wafers and silicon wafers with varying amounts of photo-resist coverage of the surface (20%, 80% and 100%). In C_2F_6 discharges CF_3^+ was consistently the dominant fluorocarbon ion present, in agreement with published cross sections for dissociative ionization [1,2,3,4,5,6]. Smaller, concentrations of CF^+, CF_2^+, and $C_2F_5^+$, were also observed, though the dissociative ionization production of $C_2F_5^+$ was a factor of five smaller than would be expected from published cross section values. The presence of photo-resist, even in small amounts, was found to produce marked changes in the discharge composition. For example in C_2F_6 discharges, concentrations of SiF_x etch products relative to concentrations of C_xF_y species were notably diminished and larger concentrations of water vapor were observed when resist was present. In CHF_3 discharges, CF_3^+ and CHF_2^+ were found to be the main species present, along with smaller concentrations of CF_2^+, CF^+, CHF^+, CH^+ and F^+.

+ Work supported by SEMATECH, by Sandia National Laboratories and by the US Dept. of Energy under contract DE-AC04-94AL85000

DISCLAIMER

I Introduction

Fluorocarbon plasmas are commonly used for etching silicon and silicon-dioxide in patterning integrated circuits. Gases such as C_2F_6 and CHF_3 are used to generate discharges rich in fluorine radicals which react at the wafer surface to form volatile fluorides of silicon. Numerous computational models have been developed to simulate such discharges. Each requires a detailed reaction database that includes cross-sections for ionization, dissociation and dissociative ionization of the process gas molecules. The published literature on CHF_3 and C_2F_6 contains a range of values for relative yields of dissociative ionization products, for reaction threshold energies, and for reaction cross sections [1-6,7,8,9,10,11,12,13]. The present work is aimed at aiding model validation efforts by providing measurements of relative ion and neutral species concentrations within reactive gas discharges used for dielectric etch. Quadrupole mass spectroscopy was used to study effects of power, pressure and substrate material (silicon or photoresist) on the composition of dielectric etch discharges. Appearance potential measurements of threshold energies and ion yields for electron impact reactions with C_2F_6 and CHF_3 molecules were also made and results compared to values expected from cross-section found in the published literature [2-13].

II Experimental Configuration and Reactor Operating Conditions

A schematic diagram of the experimental configuration is shown in Figure 1 and the GEC reactor utilized is described in detail elsewhere [14,15,16,17,18]. The effects of varying input power and chamber pressure on reactive species and etch product concentrations in C_2F_6 and CHF_3 discharges were studied. Chamber pressures was varied from 5 to 30 mTorr at a fixed inductively coupled plasma (ICP) power of 200 W, and input power was varied from 100 W to 350 W while chamber pressure was held fixed at 10 mTorr. Analysis of reflected power indicates that roughly 80% of the input power was coupled directly to the plasma, consistent with previous measurements made for Ar and Cl_2 discharges [14,15,17]. All measurements were made using 15 cm silicon wafers with 20 W bias. The wafer surface exposed to the plasma consisted of silicon, photo-resist (Shiply 1818) or combinations of these two.

A Hiden Analytical EQP mass spectrometer was mounted on one of the chamber's radial ports as shown in Figure 1. A worm drive bellows system allowed the probe tip to be positioned approximately one centimeter beyond the radial edge of the lower electrode (r=17.5cm). This distance was sufficient to prevent the plasma from attaching itself to the probe tip. The sampling orifice of the probe was positioned midway between the lower electrode surface and the bottom of the plasma confinement enhancing quartz annulus mounted below the reactor's upper quartz window [18]. The orifice separating the gas analysis chamber of the mass spectrometer from the reactor volume had diameter of either 50 μm or 100 μm. The probe interior was differentially pumped and held near 2×10^{-7} Torr in order to minimize interactions with interior surfaces.

Positive ions were extracted from the plasma by applying a potential bias of –20 V to the orifice. In this mode of operation, the filaments that generate the probe's analysis electron beam were turned off. Extracted ions were accelerated into the quadrupole sector where the mass of each was identified. The measured signal intensities directly reflect the concentrations of positive ions present within the discharge.

Neutral gas analyses, on the other hand, tends to be more complicated. Neutral atoms or molecules streaming through the entrance orifice are ionized within the filament/cage region of the probe by collisions with electrons of well-defined energy. The probe detects ions formed either from dissociative ionization of molecules or from direct ionization of atoms or molecules. Additional data analysis is then required to estimate, for example, the relative contributions to the measured CF_3^+ signal from dissociative ionization of C_2F_6 and from direct ionization of CF_3 neutral molecules produced in the reactor discharge. In an attempt to isolate the various processes involved, measurements were made in each working gas with and without a discharge present. With no discharge present, signal intensities for each ion as a function of incident electron beam energy, derived from the chamber fill gas, reflect relative reaction product yields from dissociative ionization of the parent gas molecule and allow evaluation of the threshold for each reaction.

III Experimental Results

III.1 Appearance Potential Measurements

The energy of the probe's analysis beam electrons used to initiate molecular dissociation and dissociative ionization can be controlled with an accuracy of ± 0.5 eV. Charged species generated within the probe are accelerated by a small potential difference (3 eV) into the quadrupole sector for mass analysis. Charged daughter products produced by dissociative ionization of CHF_3 and C_2F_6 are listed in Table 1 along with threshold energies for the various reactions. For our appearance potential measurements of reaction thresholds, the reactor chamber was filled with either CHF_3 or C_2F_6 gas at 10 mTorr without a discharge present. As the energy of the probe's electron beam was systematically increased from 0 to 70 eV, signals for dissociative ionization products "appeared" as the beam energy exceeded the reaction threshold. Relative yields from "appearance potential" measurements in CHF_3 and C_2F_6 are plotted in the Figures 2a and 2b respectively. In these measurements, all factors influencing the reaction rate for dissociative ionization were carefully controlled. The flux of molecules entering the probe's analysis volume was fixed by the reactor chamber pressure and the diameter of the sampling orifice. Both the energy and intensity of the analysis electron beam were defined by operational settings within the Hiden EQP probe. Consequently, the data plotted in Figure 2 reflects not only of the reaction energy thresholds, but also the relative magnitudes of dissociative ionization cross-sections for the various reaction products observed.

As shown in Figure 2a, we find dissociative ionization reaction products from CHF_3, in order of decreasing intensity, to be CF_3^+, CHF_2^+, CF^+, CF_2^+, CHF^+, F^+ and CH^+. Within the scant published literature on CHF_3 dissociative ionization, there are discrepancies in values reported for reaction thresholds, cross-sections and relative yields. Comparisons of the published data with our results are provided in Tables 1 and 2. Thresholds measured for production of CF_3^+, CF_2^+, CF^+, CH^+, and F^+ from CHF_3 are in good agreement with previously published results, while those for CHF^+_2 and CHF^+ production are found to be lower than previously reported. Appearance potential thresholds for electron impact ionization of C_2F_6 are found to be consistent with previously reported values though equipment problems led to larger than normal error bars for measurements in this gas. We plan to repeat C_2F_6 appearance potential measurements at the next opportunity.

Measurements of dissociative ionization product yields from CHF_3 and C_2F_6 as a function of incident electron energy are shown as in Figures 2a and 2b, respectively. For CHF_3, we find CF_3^+ and CHF_2^+ to be the principal dissociative ionization products, followed by smaller yields for CF^+, CF_2^+, CHF^+, F^+ and CH^+. Yield intensities observed for CF_3^+, CF_2^+ and CF^+ agree well with those reported by Jiao [8] et al., however, the large yield for CHF_2^+ reported by Jiao is not observed, see Table 2. The large relative yield for CF^+ reported by Poll and Meichsner [9] and by Goto et al. [10] is also not observed. Measurements of dissociative ionization products from C_2F_6 as a function of incident electron energy are shown as in Figure 2b. In this case, we found CF_3^+ to be the principal product, followed by CF^+, $C_2F_5^+$ and CF_2^+. The relative intensities of the C_2F_6 product yields observed for CF_3^+, CF^+, and CF_2^+ are consistent with cross section values reported in [1,2]. However, the observed yield for $C_2F_5^+$ is about five times smaller than expected from these cross-sections. Work is in progress to assess the sensitivity of computational models of dielectric etch reactor operation to the variations in thresholds and yields discussed above.

III.2 Dielectric Etch Reactor Operation With C_2F_6

Neutral Gas Analysis

When a discharge is initiated in C_2F_6 gas, signals observed with the EQP operating in neutral gas analysis mode could result from two reaction pathways. Ions detected could result from dissociative ionization of C_2F_6 molecules which enter the probe, or from direct ionization of molecules such as CF_3, CF_2, and CF previously produced in the reactor. For reactor operation at 200 W, 10 mTorr, and 20 W bias on a silicon wafer substrate, Figure 3 shows C_2F_6 daughter molecules and silicon etch products detected. Principally, in order of decreasing intensity, we observed CF_3^+, SiF_3^+ and SiF_2^+, along with small signals for CF^+, CF_2^+ and $C_2F_5^+$. In addition, we observed a strong signal for H_2O^+, as well as signals for CO^+, CO_2^+ and OH^+, all of which result from residual resist products and residual water vapor in the reactor chamber. Silicon etch products detected were in the form of SiF_2^+ and SiF_3^+. No signals were detected for F^+ or Si^+, indicating no accumulations of neutral atomic fluorine or silicon within the reactor.

The presence of photoresist, even in small amounts, resulted in a significant increase in the signal for H_2O^+ as shown in Figure 4. H_2O^+ concentrations remained high, but decreased slightly,

as resist coverage on the wafer was further increased from 20% to 100%. The presence of resist also resulted in sharp decreases in the relative concentrations of both CF_x^+ and SiF_x^+ species as shown in Figure 4. We postulate that the additional rise in water vapor results from interaction of hydrogen introduced by the resist with oxygen liberated from the quartz annulus used to confine the discharge. Experiments with controlled injection of oxygen and hydrogen gas, with and without resist present, are planned to further elucidate the reaction mechanisms involved. In Figure 4, the small increases in CF_x^+ signals and small decrease in H_2O^+ signals at 100% resist coverage are thought to be due to the age of the resist coating for that particular wafer. Fresh resist coatings were deposited for measurements at 20% and 80% resist coverage. The blanket resist wafer used had been stored for more than a month and curing seems to have reduced the residual hydrogen content of this particular film.

Positive Ion Analysis

The masses of positive ions extracted from the reactor while operating with C_2F_6 are plotted in Figure 5. For C_2F_6, the principal positive ions detected in order of decreasing concentration were CF_3^+, CF^+, CF_2^+, $C_2F_5^+$, SiF_3^+, CO^+, $C_2F_4^+$, SiF^+, and SiF_2^+. In contrast to neutral gas analysis, interpretation of data collected in EQP ion analysis mode is straight forward. Because the electron analysis beam inside the probe is turned off, signals measured directly reflect the relative concentrations of ions within the reactor. For silicon wafer substrates, CF_3^+ was the principal ion within the reactor discharge. Concentrations of other fluorocarbon ions and of silicon etch products are smaller, as shown in Figure 5a. Concentrations of positive ions within the reactor during operation at 200 W power, 10 mTorr pressure, and with a wafer surface composed of 20% resist and 80% silicon are plotted in Figure 5b. Although large concentrations of H_2O^+ were detected during EQP neutral gas analysis, no H_2O^+ ions were detected within the discharge. This indicates that electron energies within the reactor are below the 12.56 eV threshold required to ionize water molecules. CF_x^+ species with x=1 and 3 were the principal positive ions detected. No signals for SiF_x^+ were found although 80% of the surface exposed to the discharge was silicon. The data in Figure 6 shows that the discharge ion fraction of CF^+ increases when resist is present, while

relative populations of other fluorinated ions decrease. These modifications could be the result of changes in the gas-phase species present and/or of changes in the electron energy distribution function produced by repartition of the available energy among the available reaction pathways. Again, data for reactor operation with blanket resist coverage (100%) appears to be affected by the age of that particular resist film.

Concentrations of positive ions collected as a function of pressure during C_2F_6 reactor operation are shown in Figure 7a. Concentrations of each species increase between 3 and 15 mTorr. At pressure is increased from 20 – 30 mTorr, ion concentrations detected diminish. The dependence of ion concentration on pressure at fixed reactor power, shown in Figure 7a for C_2F_6 discharges, is typical of that observed for CHF_3 discharges and for metal etch discharges using Cl_2 and BCl_3 gas mixtures [19]. The reduced ion concentrations at larger pressures may result from a reduction in electron temperature due to increased collisions. The observed behavior could also be due to reduction in the radial extent of the cylindrical plasma with increasing pressure. Radial compression of the discharge volume has been previously observed for some GEC discharges. This would cause an increase in the distance between the plasma boundary and the probe's collection orifice, thus lowering the intensity of the ion currents collected. Langmuir probe measurements of ion saturation current, I_{sat}, completed to date, are roughly consistent with the behavior shown in Figure 7a. For Cl_2/BCl_3 (2:1) discharges operated at a total gas flow of 10 sccm and ICP power of 300 W, the ion saturation current at the center of the reactor was unchanged for pressures of 10 and 40 mTorr. Closer to the edge of the discharge at r = 6 cm, an I_{sat} value of 0.19 mA was measured at 10 mTorr, while I_{sat} = 0.13 mA at 40 mTorr. These Langmuir probe results were obtained during reactor operation without the quartz confinement ring shown in Figure 1 and data have not been collected over the entire pressure range between 5 and 30 mTorr. In future experiments, we plan to use a multi-tipped Langmuir probe to measure the radial dependence of ion density within the reactor as a function of pressure.

Figure 7b shows that concentrations of all ion species produced in the reactor increase as power was raised from 100 to 250 W. For a few species, CF_3^+, CF_2^+, CF^+, and CO^+,

concentrations were observed to decrease between 250 and 350 W again, for reasons that are not fully understood at this time. Langmuir probe measurements of electron density and temperature planned during the next phase of experiments will provide additional insight. Signal intensity of other ion species like, SiF^+, SiF_3^+ and $C_2F_5^+$, continue to increase with increasing power. The rate of increase for CF_3^+ concentration is notably larger than that observed for all other species as power was increased from 100 to 300 W. Similar behavior of ion species concentration with power was observed for CHF_3 etch discharges and for BCl_3/Cl_2 metal etch discharges [19].

III.3 Dielectric Etch Reactor Operation With CHF_3

Neutral Gas Analysis

Figure 8a shows the species detected with the EQP probe operating in neutral gas analysis mode during reactor operation with CHF_3. Frequent exposure of the reactor chamber to ambient while changing wafers resulted in a strong signal for H_2O^+ at mass 18 amu. The intensity of the signal for HF^+ also increased significantly when the discharge was turned on. Published literature for dissociative ionization of CHF_3 [7-13] does not include reactions for formation of HF, and it is possible that HF is being formed by reactions of radical fluorine molecules with the water vapor present. Signal intensities for CF_3^+, CF_2^+, CHF_2^+ and CF^+ decrease significantly when the discharge was initiated, which may reflect a decrease in the partial pressure of CHF_3 due to dissociation by the discharge. Figure 8b shows the intensities of signals detected at each mass during EQP neutral gas analysis for a 200 W ICP power, 20 W bias, 10 mTorr discharge with a blanket resist wafer substrate. In the presence of resist, the water vapor signal increased considerably, and its relative abundance was well above the residual water vapor concentration shown in Figure 8a. As expected, SiF_x species were not detected for the blanket resist wafer. When the pressure was increased from 5 to 25 mTorr with all other reactor parameters unchanged, signals for CF_3^+, CHF_2^+, CF^+, and CF_2^+ increase linearly. Similar behavior was observed for C_2F_6 daughter products during reactor operation with wafers having 20%, 80% and 100% resist surface coverage. In each case, signals for H_2O^+, OH^+ and CO_2^+ were constant with pressure indicating a water vapor source independent of the primary gas feed. When pressure and bias power were held

constant at 10 mTorr and 20 W. signals for H_2O^+, OH^+, CO^+ and CO_2^+ were again nearly unchanged as ICP power was varied between 100 and 300 W. At the same time, signals for CF_3^+, CHF_2^+, CF^+, and CF_2^+ were found to decrease with increasing power demonstrating behavior similar to that shown in Figure 7b for C_2F_6.

Positive Ion Analysis

Positive ion concentrations in CHF_3 discharge at chamber pressure of 10 mTorr, 200 W ICP power, 20 W bias on a silicon wafer substrate are shown in Figure 9a. CHF_2^+ was the largest ion concentration detected. with smaller concentrations observed for CF_3^+, CF_2^+, CF^+, CO^+ and HF^+. Etch product ions detected were principally SiF^+ and SiF_3^+. At constant power, currents of positive ions extracted from the discharge increase with chamber pressure for pressures below 20 mTorr. At pressures in excess of 20 mTorr, the extracted positive ion currents dropped with increasing pressure, demonstrating behavior similar to that shown in Figure 7a for C_2F_6 discharges and also observed in Cl_2/BCl_3 metal etch discharges [19]. At a pressure of 10 mTorr, ion currents extracted from the reactor peak at ICP power levels near 100-150 W. As discussed above, smaller currents collected at higher powers could reflect a decrease in the plasma radius.

For discharges operated with blanket resist wafers the fraction of CHF_2^+ ions within the discharge decreased, even though the resist introduces additional hydrogen, while those for CF^+, CF_3^+ and CF_2^+ increase, as shown in Figures 9. It is interesting that in the presence of resist concentration s of CF_2^+ were the largest. while for operation with blanket silicon wafers CF_2^+ concentrations were found to be fourth largest, behind those of CHF_3^+, CF_3^+ and CF^+. The observed relative abundance of each of these ionic species in presence of a silicon wafer is consistent with the fractional yields for dissociative ionization shown in Figure 2a. The yield for CF_2^+ is about a factor of ten below that of CF_3^+, while those for CF^+ and CHF_2^+ are roughly evenly distributed between these two. The prevalence of CF_2^+ in CHF_3 discharges in the presence of resist indicates changes in the reaction pathways for formation of all $C_xH_yF_z$ neutral molecules and ions. Improved understanding of such processes is essential if databases enabling accurate computer simulation of dielectric etch discharges are to be compiled.

IV Summary and Conclusions

Mass spectrometric analysis was performed to determine the reactive species present in dielectric etch reactors operating with C_2F_6 and CHF_3. Uncollided beams of neutral species within the reactor were collected and analyzed before interactions with material surfaces could take place. Potential bias extraction of ions from the reactor volume allowed for direct measurements of the species present and their relative concentrations. Appearance potential measurements made on the background fill gas with no discharge present allowed determination of relative dissociative ionization yields and of reaction threshold energies. For C_2F_6 thresholds and yields observed for all dissociative ionization products except $C_2F_5^+$ agreed well with cross-section values previously published [1,2]. The yield for $C_2F_5^+$ was found to be five times smaller than previously reported, assuming constant collection efficiencies for each product within our probe. Considerable confusion exists within the published literature on dissociative ionization of CHF_3 [7-10], with little agreement even on which products are most prevalent. Measurements on neutral gas reported here provide additional estimates of the relative yields and reaction thresholds, though we are unable to provide quantitative cross-section values.

Charged and neutral reactive species concentrations were measured for reactor operation with different wafer surface materials including blanket silicon, blanket resist, and combinations of these two. In C_2F_6 discharges with blanket silicon wafers, CF_3^+ was by far the ion with largest concentration. Notable concentrations of SiF_x^+ species were also detected. Silicon molecules detected do not necessarily represent volatile products evolving from the wafer as the measurements detect these ions in the plasma volume away form the wafer surface. Ions observed are most likely formed in subsequent reactions occurring within the discharge volume. Introduction of small amounts of photoresist onto the wafer surface resulted in marked changes in ion concentrations within the discharge. For C_2F_6 discharges, CF_3^+ populations dropped significantly, CF^+ became the dominant ion, and concentrations of SiF_x^+ species were diminished. Similar behavior was observed for etch reactor operation with CHF_3.

Acknowledgments: Our thanks to Thomas Hamilton at Sandia Labs for help with experiments, and to Vince McKoy and Justine Johannes for useful discussions and background material.

Table 1 : Dissociative Ionization Reactions for C_2F_6 and CHF_3

Dissociative Ionization Reactions for CHF_3	Threshold Energy (eV)	Reference
$CHF_3 + e \rightarrow CF_3^+ + H + 2e$	13.70 – 15.20 14.7 ± 1.0	[7, 10-13] this work
$CHF_3 + e \rightarrow CHF_2^+ + F + 2e$	16.40 – 16.80 14.3 ± 1.0	[7, 10-12] this work
$CHF_3 + e \rightarrow CF_2^+ + HF + 2e$ $\rightarrow CF_2^+ + H + F^- + e$	17.50 – 21.20 15.7 ± 1.0	[7,10,11,13] this work
$CHF_3 + e \rightarrow CHF^+ + F_2 + 2e$	19.80 13.5 ± 1.0	[10] this work
$CHF_3 + e \rightarrow CF^+ + HF + F + 2e$	20.20 – 21.60 19.5 ± 1.0	[7,10,11,13] this work
$CHF_3 + e \rightarrow CH^+ + F_2 + F + 2e$	33.50 31.3 ± 1.0	[10] this work
$CHF_3 + e \rightarrow F^+ + \ldots$	37.00 37.3 ± 1.0	[10] this work

Dissociative Ionization Reactions for C_2F_6		Threshold (eV) Theory McKoy et al. [2]	Experiments [3-6]	appearance potential
$C_2F_6 + e^- \rightarrow$	$C_2F_6^+ + 2e^-$	14.46	13.40	
	$CF_3^+ + CF_3 + 2e^-$	12.83	13.32	16 ± 3
	$CF_2^+ + CF_4 + 2e^-$	13.15	13.53	18 ± 3
	$C_2F_5^+ + F + 2e^-$	14.31	14.74	18 ± 3
	$CF_3^+ + CF_2 + F + 2e^-$	16.54	17.08	
	$C_2F_4^+ + F_2 + 2e^-$	17.66	17.19	
	$CF^+ + CF_3 + F_2 + 2e^-$	20.61	20.84	18 ± 3
	$C_2F_5 + F^+ + 2e^-$	23.19	22.91	
	$C_2F_3^+ + 2F_2 + 2e^-$	25.23	25.32	

Table 2: Reaction Product Yields For Dissociative Ionization Of CHF_3

Product	Cross-section (10^{-20} m^2)			Relative Intensity
	Poll & Meichsner [9] E = 70eV	Goto et al. [10] E = 70eV	Jiao, et al [8] E = 60eV	This Work E = 70eV
CF_3^+	1.28	2.04	0.95	1.000
CHF_2^+		0.41	1.80	0.900
CF_2^+		0.17	0.20	0.200
CF^+	2.52	2.50	0.51	0.500
CHF^+		0.42		0.080
F^+		0.10		0.010
CH^+		0.02		0.003

References

[1] G. Christophourou and J. K. Olthoff, J. Phys. Chem. Ref. Data **27**, No. 1, 1, (1998).

[2] V. McKoy, Bul. Amer. Phys. Soc. **43**, No. 5, 1473, (1998).

[3] S. G. Lias, J. E. Bartmess, J. F. Liebmann, J. L. Holmes, R. D. Levin, and W. G. Mallard, J. Phys. Chem. Ref. Data. **17**, Suppl. 1, (1998).

[4] M.W. Chase, C.A. Davies, J.R. Downey, D.J. Frurip, R.A. McDonald, and A.N. Syverud, JANF Thermochem. Tables, Third Ed., J. Phys. Chem. Ref. Data. 14, Suppl. 1, (1985).

[5] I. Barin, *Thermochemical Data of Pure Substances*, Third Ed., VCH, Weinheim, (1995).

[6] R. L. Asher and B. Rusic, J. Chem. Phys., **106**. 210, (1997).

[7] G. Christophourou , J.K. Olthoff and M.V.V.S. Rao, J. Phys. Chem. Ref. Data. **26**, No. 1, 1, (1997).

[8] Q. Jiao, R. Nagpal and P. D. Haaland, Chem. Phys. Lett., **269**, 117, (1997).

[9] H.U. Poll and J. Meichsner, Contrib. Plas. Phys. **27**, 359, (1987).

[10] M. Goto, K Nakamura, H. Toyoda and H. Sugai, Jpn. J. Appl. Phys. **33**, 3602, (1994).

[11] D. L. Hobrock and R. W. Kiserr, J. Phys. Chem. **68**, 575, (1964).

[12] J.B. Framer, I.H.S. Henderson, F.P. Lossing, and D.G.H. Marsden, J. Chem. Phys. **28**, 348, (1956).

[13] C. Lifshitz and F. A. Long, J. Phys. Chem. **69**, 3731, (1965).

[14] G.A. Hebner, J. Appl. Phys. **81** (2), 578, (1997).

[15] G.A. Hebner, J. Vac. Sci. Technol. A **14**, (4), 2158, (1996).

[16] C.B. Fledderman and G.A. Hebner, J. Vac. Sci. Technol. A **14**, (4), 1955, (1997).

[17] P. A. Miller, J. Res. National Inst. of Stand. & Tech. **100**, 427, (1995).

[18] H.M. Anderson and L. Perry, Bul. Amer. Phys. Soc. **43**, No. 5, 1411, (1998).

[19] R. Jayaraman, R.T. McGrath, G. Hebner and J.A. Sherwin, Bul. Amer. Phys. Soc. **43**, No. 5, 1459, (1998).

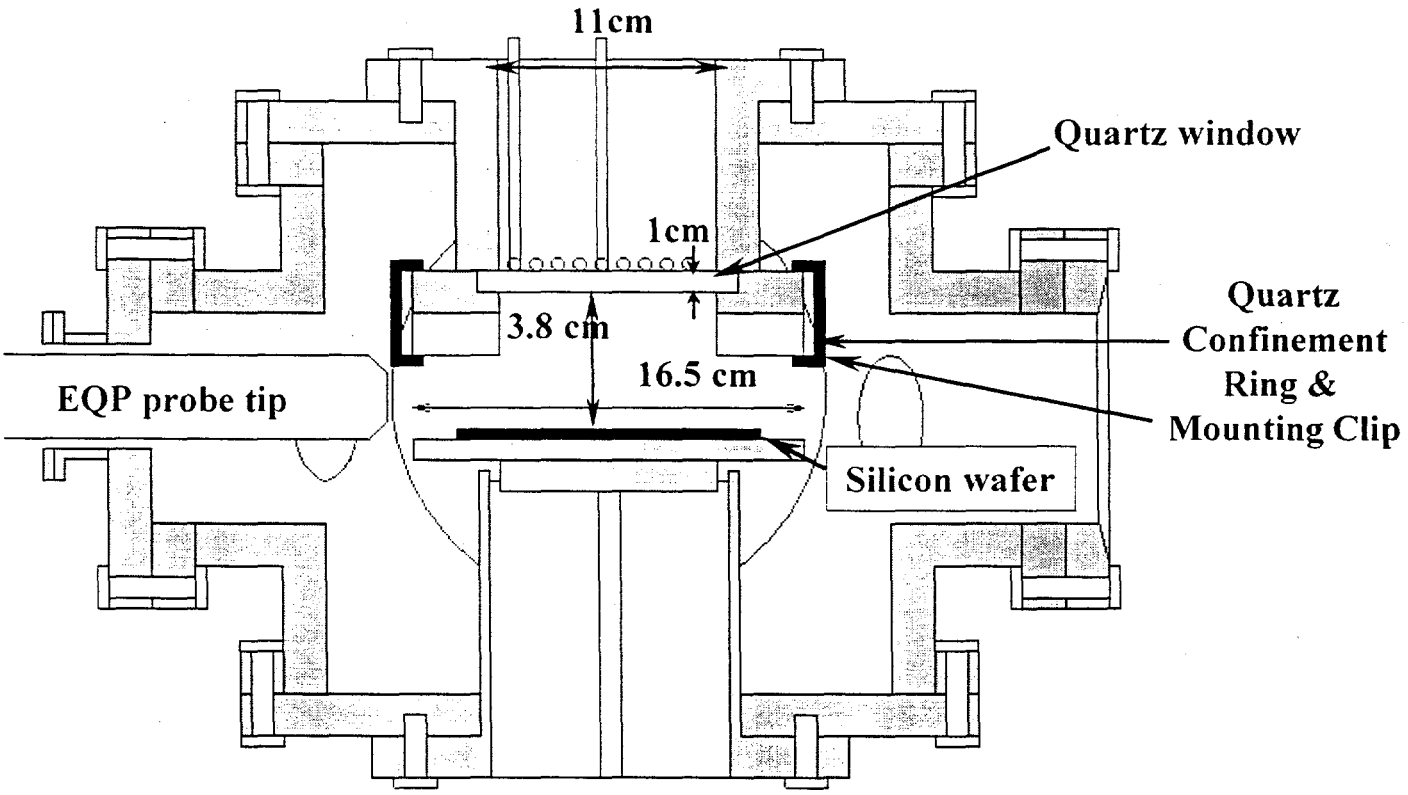

Figure 1 - Schematic diagram of Sandia's inductively coupled GEC research reactor chamber.

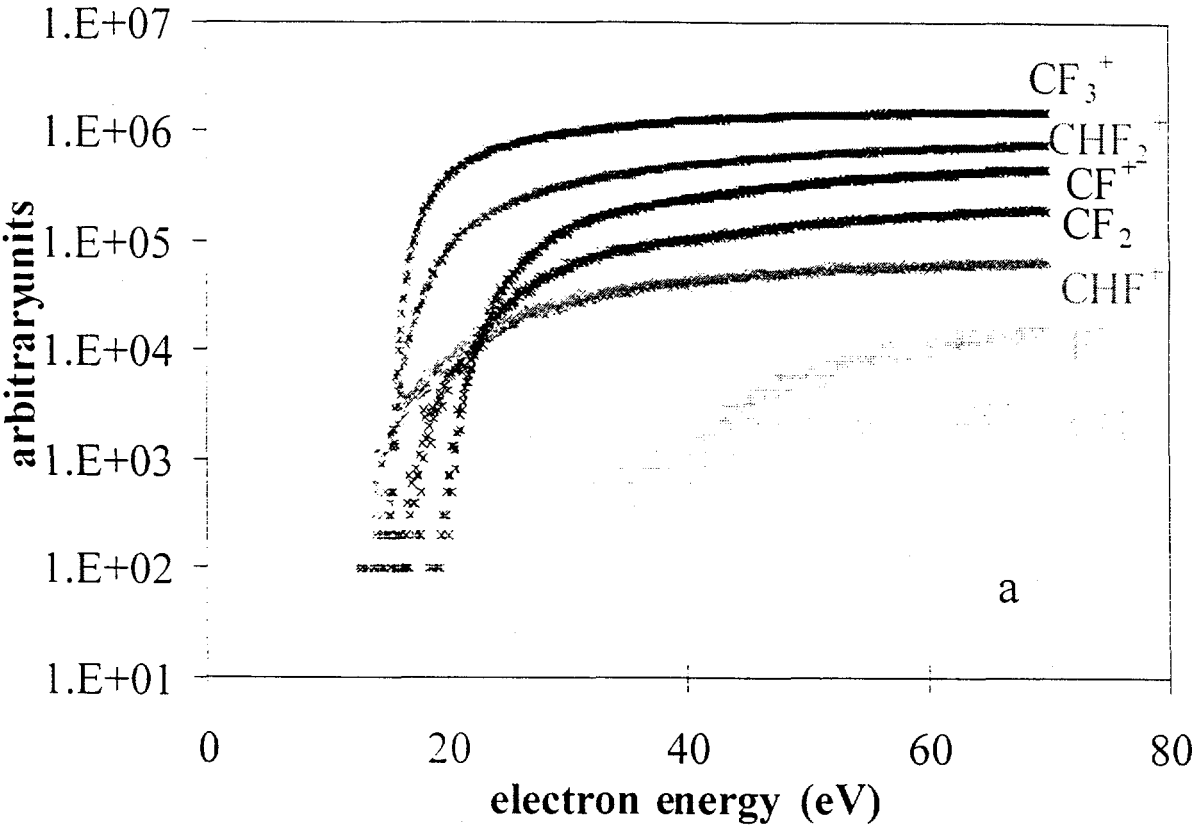

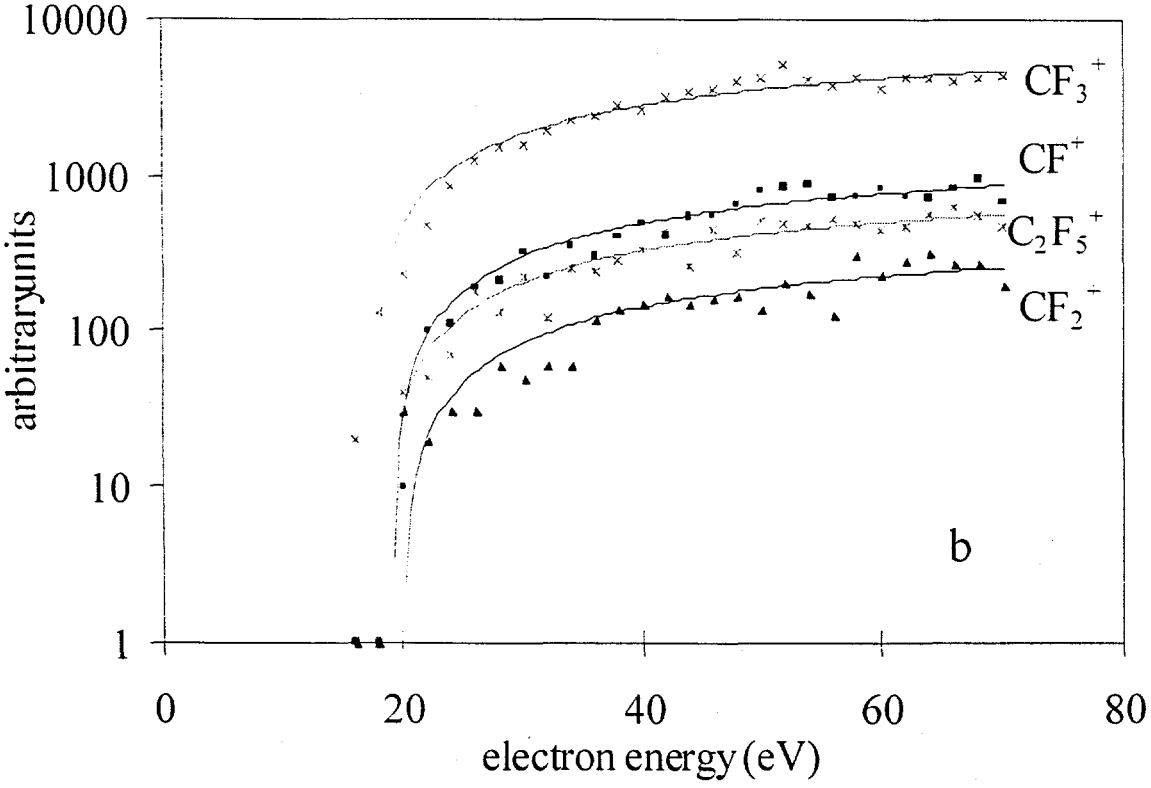

Figure 2 - Appearance potentials for dissociative ionization of a) CHF_3 and of b) C_2F_6 showing charged product yields as a function of incident electron beam energy.

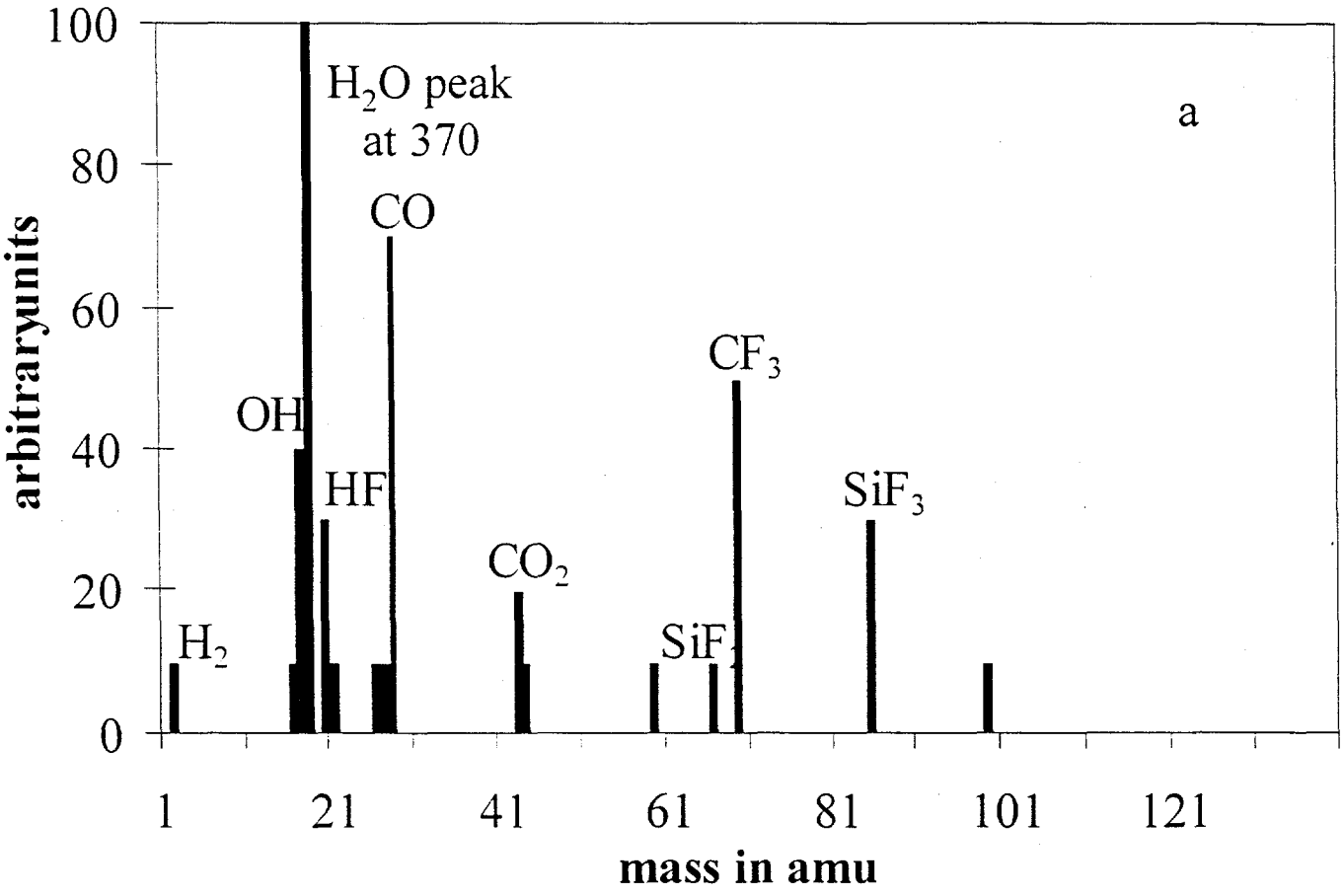

Figure 3 - Neutral species detected in C_2F_6 discharges at 200 W power, 10 mTorr pressure and 20 W bias with a blanket (100%) silicon wafer surface.

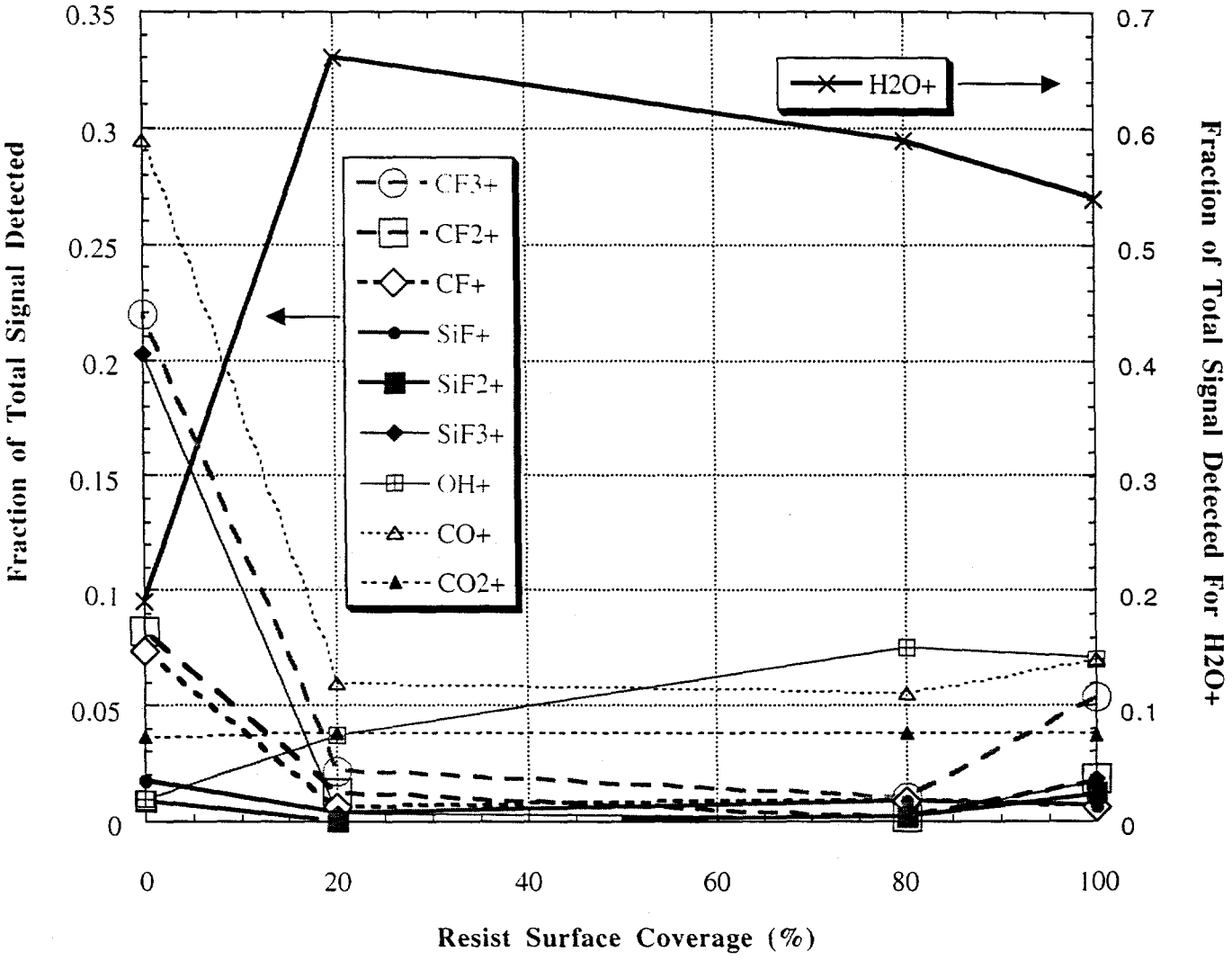

Figure 4 - Fractions of total signal for each species detected during EQP neutral gas analysis as a function of resist surface coverage on the silicon wafer. Reactor operation was at 200 W power, 10 mTorr pressure of C_2F_6 and 20 W bias.

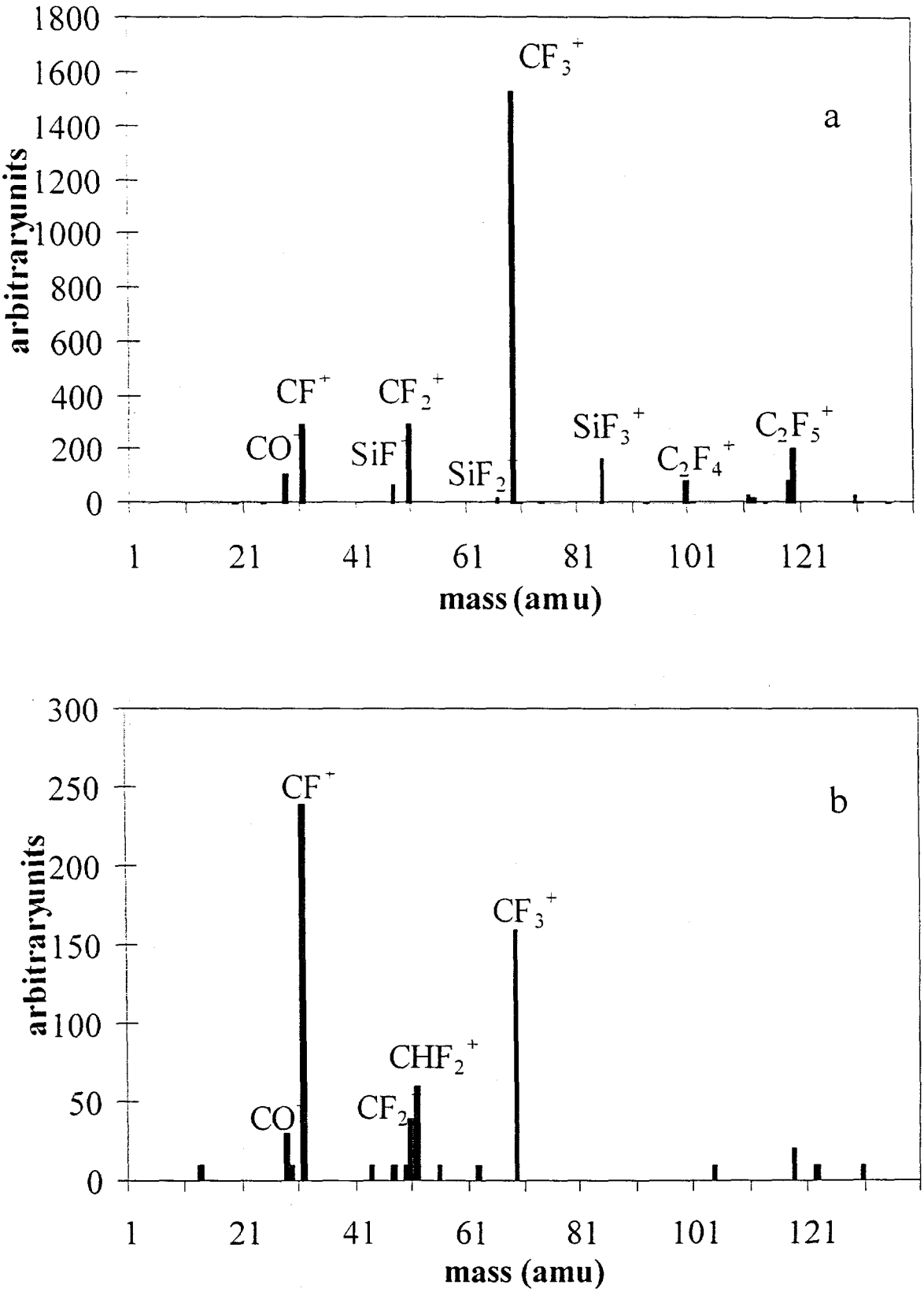

Figure 5 - Positive ions detected in C_2F_6 discharges at 200 W power, 10 mTorr pressure and 20 W bias on a) silicon wafer substrate b) resist covered (20% of surface) silicon wafer.

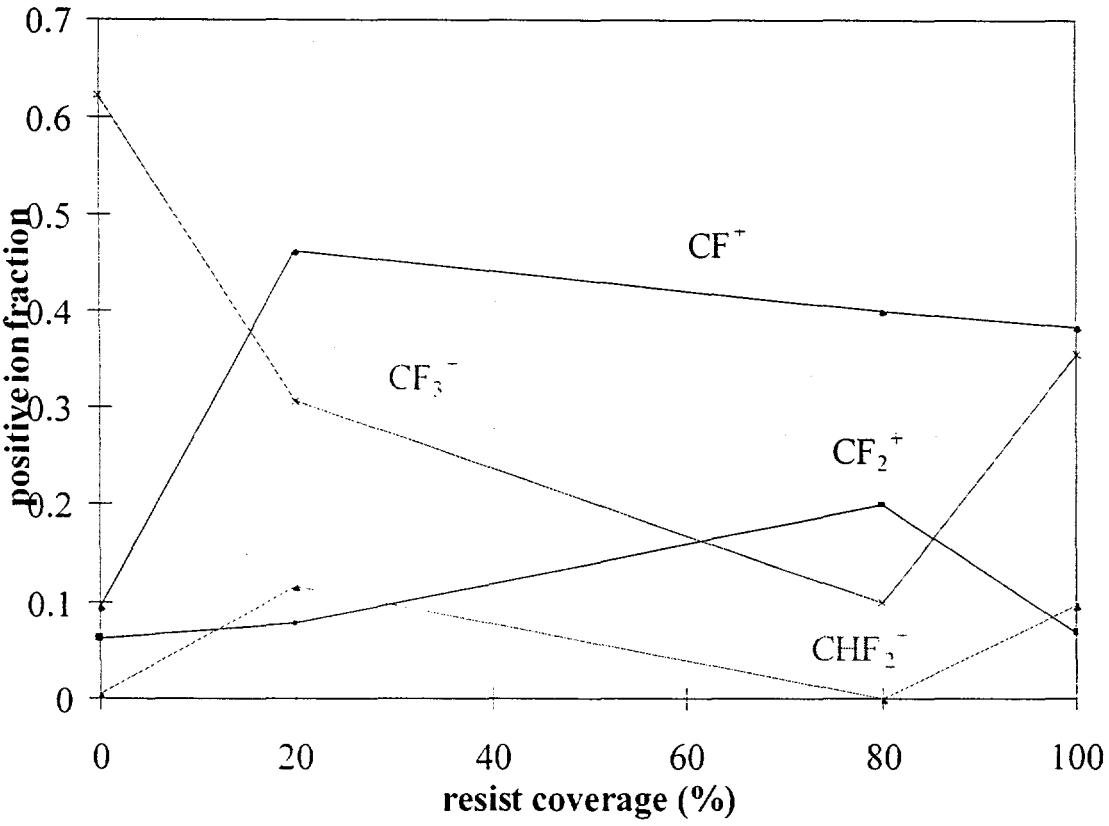

Figure 6 - CF_x^+ fractions as a function of percentage resist surface coverage on silicon wafers for reactor operation at 200 W power, 10 mTorr C_2F_6 pressure and 20 W bias.

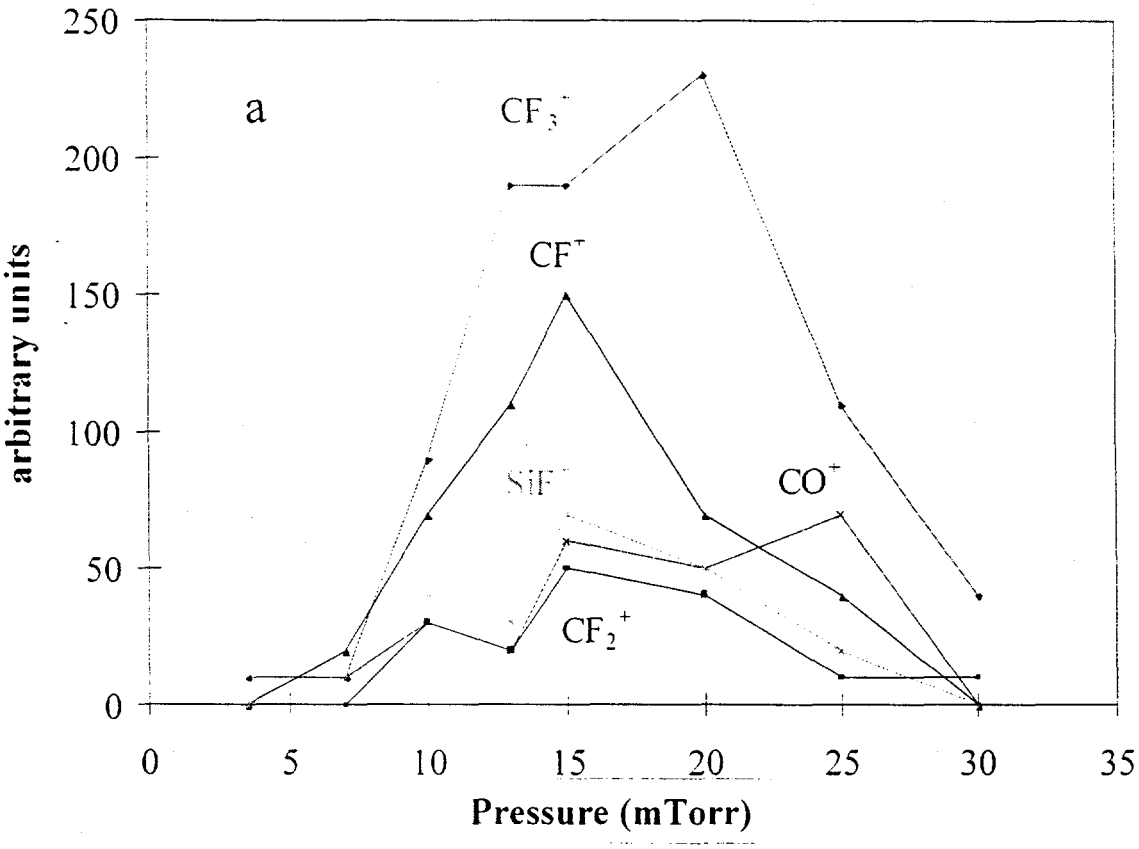

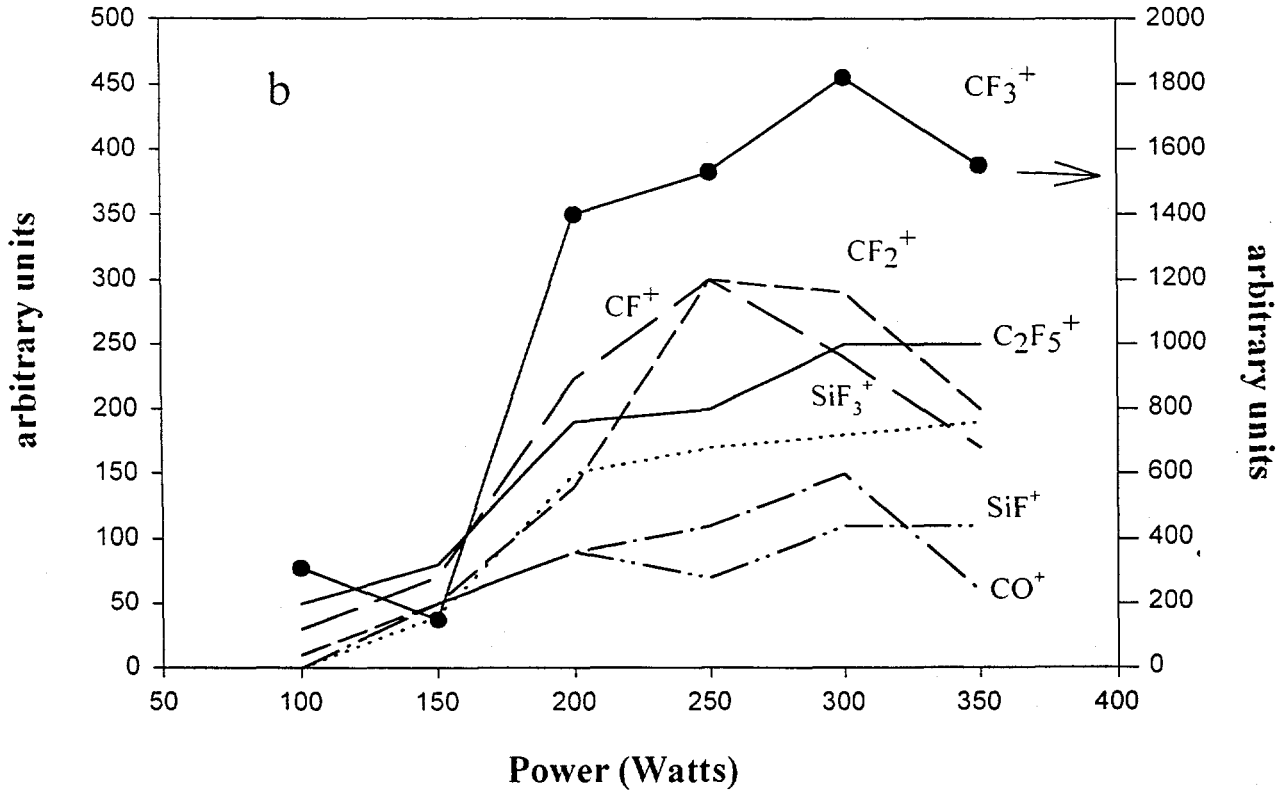

Figure 7 - Positive ions detected in C_2F_6 discharges with 20 W bias on silicon substrate a) as a function of pressure at 200 W power b) as a function of power at 10 mTorr pressure.

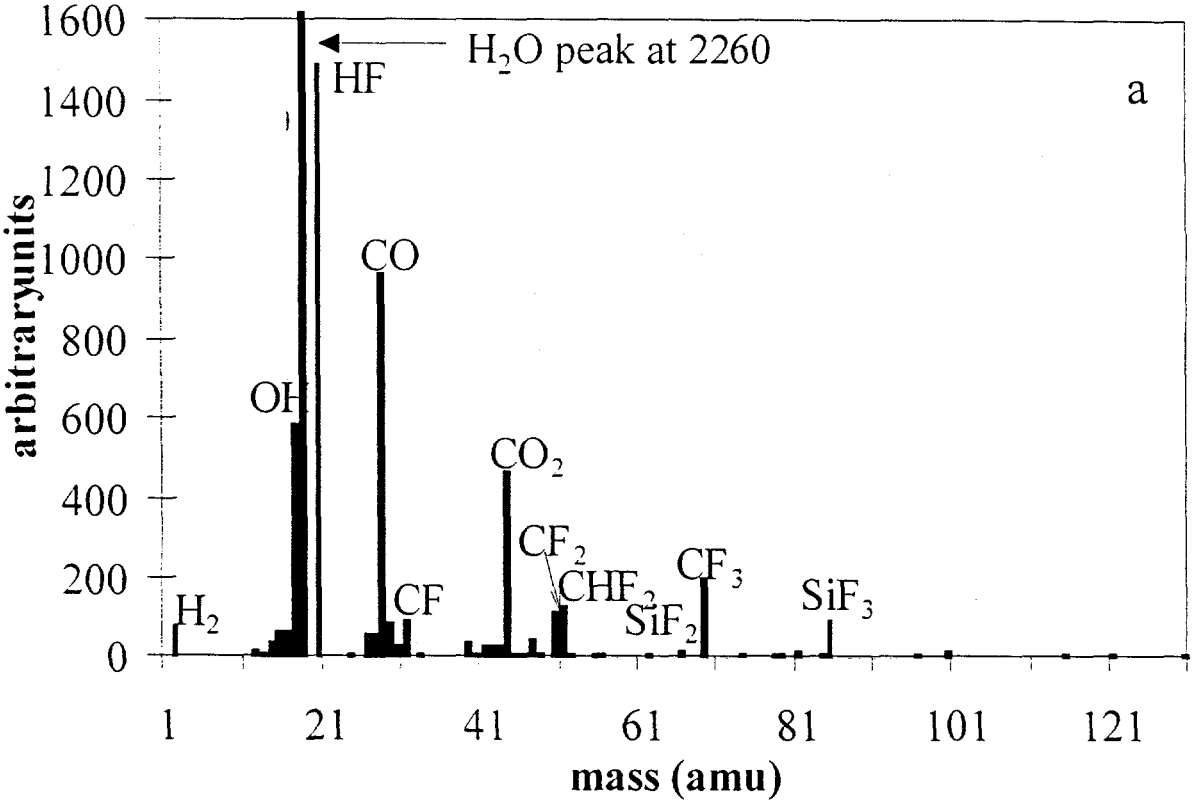

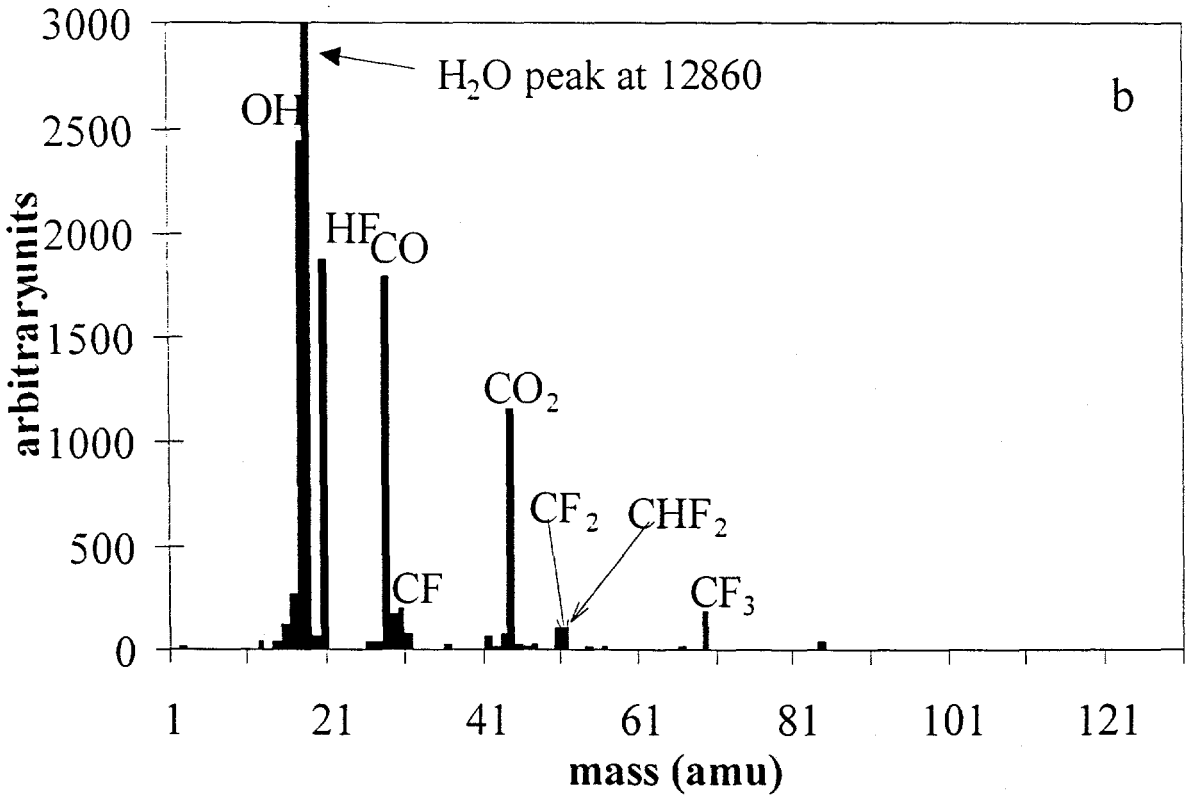

Figure 8 - Neutral species detected in CHF_3 discharge at 200 W power, 10 mTorr pressure and 20 W bias for reactor operation with a) a silicon wafer substrate, and b) a blanket resist covered silicon wafer substrate.

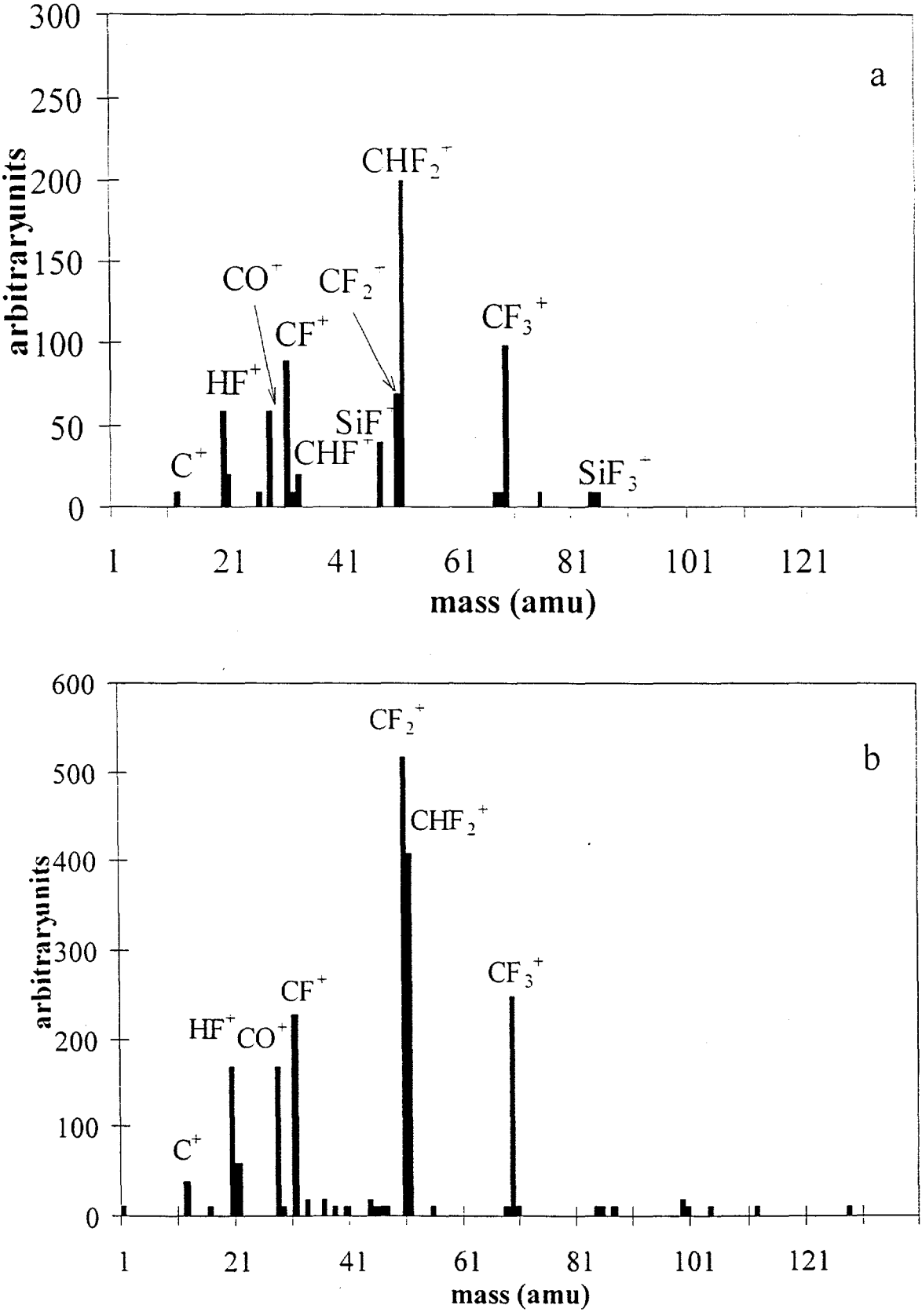

Figure 9 - Positive ions detected in CHF_3 discharges at 200 W power. 10 mTorr pressure and 20 W bias with a) a silicon wafer substrate and b) a blanket resist covered silicon wafer.